

NON-HARMONIC ANALYSIS BASED INSTANTANEOUS HEART RATE ESTIMATION FROM PHOTOPLETHYSMOGRAPHY

Fangyu Li[†], WenZhan Song[†], Changwei Li^{*} and Aiying Yang^{*}

[†]Center for Cyber-Physical Systems, University of Georgia

^{*}College of Public Health, University of Georgia

^{*}School of Optics and Photonics, Beijing Institute of Technology

ABSTRACT

Instantaneous Heart Rate (IHR) detection is important but challenging. As a kind of biomedical signal, photoplethysmography (PPG) is a good source to extract the intrinsic IHR information for further diagnostic interpretation. However, because of the non-stationary characteristics, the traditional IHR estimation results can be unreliable, and may be contaminated with artifacts and noises. Even state-of-art time-frequency analysis techniques can not fully handle the sub-harmonics interferences to obtain a reliable and robust IHR estimation. In this paper, we propose a hybrid IHR estimation approach based on the non-harmonic analysis (NHA) and an advanced time-periodic transform (TPT). We propose to use a NHA model to adaptively extract intrinsic oscillatory modes from PPG data. The previously unsuppressed sub-harmonic components can be removed thanks to the extracted mono-frequency components. Then the IHR can be estimated from the left ridge on TPT. Experiment results demonstrate the advantages of the proposed approach, which is promising for PPG signal processing and analysis.

Index Terms— PPG, non-harmonic analysis, oscillatory mode extraction, IHR, time-periodic analysis.

1. INTRODUCTION

Monitoring chest movements, photoplethysmography (PPG) data contain both respiratory and cardiac rhythms, reflecting human body status and health conditions [1–3]. Since the traditional harmonic analysis is not suitable for biomedical analysis [4], the non-harmonic analysis (NHA) has been an important tool for the non-stationary PPG signal analysis [5–8]. The NHA hypothesis is that a signal may contain a few of components (principle and minor) with different non-harmonic oscillation patterns [4], and NHA characterizes the non-stationary time series signal features, separates principal and minor components, and removes different kinds of interferences, such as motion artifacts [9].

Our research is partially support by NSF-CNS-1066391, NSF-CNS-0914371, NSF-CPS-1135814, NSF-CDI-1125165, and Southern Company.

Instantaneous heart rate (IHR) estimation from PPG has drawn more and more attentions [3, 10–12], which can be used for human health monitoring and heart rate turbulence detection [13]. Nevertheless, NHA does not generate promising IHR estimates, because the physical meanings of the oscillation patterns still lack of investigations [4]. In addition, biomedical signals generate sub-harmonic artifacts in the time-frequency (TF) domain. Inspired by the concept of cepstrum, Su and Wu proposed a de-shape STFT (short-time Fourier transform) [14], and Lin et al. [15] developed another advanced time-periodic transform (TPT) called de-shape SST (synchrosqueezing transform) to suppress the sub-harmonic influences. However, expect ideal cases, the interactions between different components reduces the suppression effectiveness. Although acceptable IHR results were obtained via only checking 0~2Hz, the manual “bandpass filter” is not an optimal operation for biomedical analysis.

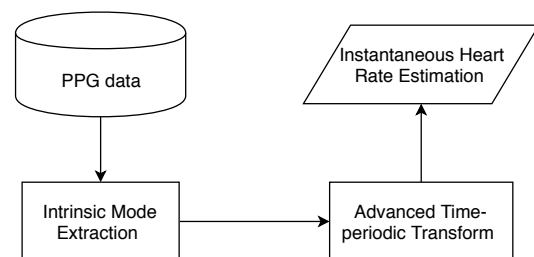


Fig. 1. The proposed workflow to estimate IHR from PPG.

In this paper, we propose a NHA based IHR estimation approach for PPG data. In our approach, as shown in Fig. 1, intrinsic oscillatory components are first adaptively extracted, then an advanced TPT is applied on the cardiac component to generate a high-resolution time-periodic representation, from which the IHR is estimated. Compared with [4] and [15], our main contributions are the following: 1) we combine the NHA and an advanced TPT technique to estimate IHR; 2) influences from the non-trivial sub-harmonics are suppressed; 3) IHR can be directly estimated without manual constraints. Finally, we demonstrate the advantages of our method via real PPG data experiments with quantitative comparisons.

2. THEORY

2.1. Non-harmonic Analysis

In NHA, a non-stationary signal $f(t)$ can be defined as a summation of K oscillatory modes [4]:

$$f(t) = \sum_{k=1}^K \alpha_k(t) s_k(2\pi N_k \phi_k(t)) + \sigma(t) r(t), \quad (1)$$

where, $\alpha_k(t)$ is the instantaneous amplitude (IA), $N_k \phi_k(t)$ is the instantaneous phase (IP) whose derivative is the instantaneous frequency (IF), $\{s_k(t)\}_{1 \leq k \leq K}$ are wave-shape functions with a unit norm, σ is a slowly varying smooth function and $r(t)$ is the residual, which is a stationary random process with unit standard deviation describing the noise.

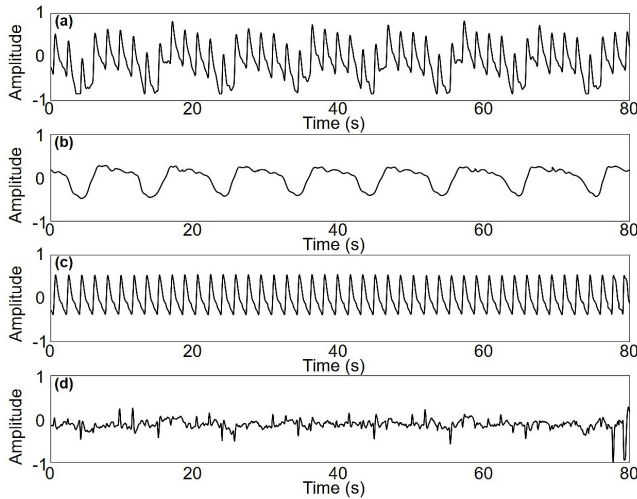


Fig. 2. Intrinsic oscillatory modes extracted from PPG. (a) Raw PPG signal; (b) Respiratory component and (c) Cardiac component (heartbeat); (d) Residual when both respiratory and cardiac components have been removed.

2.2. Intrinsic Mode Extraction

Biomedical signals, such as PPG, have time-varying amplitudes, phases, and wave-shapes. To better analyze these non-stationary time series, intrinsic mode (IM) was defined as [4]:

$$f_k(t) = \sum_{n=-N/2}^{N/2-1} a_{n,k} \cos(2\pi n \phi_k(t)) s_{cn,k}(2\pi N_k \phi_k(t)) + \sum_{n=-N/2}^{N/2-1} b_{n,k} \sin(2\pi n \phi_k(t)) s_{sn,k}(2\pi N_k \phi_k(t)), \quad (2)$$

where, $\{a_{n,k}\}$, $\{b_{n,k}\}$ are real numbers, and $\{s_{cn,k}(t)\}$ and $\{s_{sn,k}(t)\}$ are real shape function series. IM is a generalization of the model $\alpha_k(t) s_k(2\pi N_k \phi_k(t))$ in Equation (1). Because when $s_{cn,k}(t)$ and $s_{sn,k}(t)$ in Equation (2) equal to

the same wave-shape function $s_k(t)$, the model in Equation (2) is reduced to Equation (1). To calculate the IM, either the recursive diffeomorphism based regression (RDBR) algorithm [4] or the recursive diffeomorphism based spectral analysis (RDSA) algorithm [16] can be adopted. Fig. 2 shows an IM extraction example. Fig. 2a is the raw PPG signal, while Fig. 2b and Fig. 2c are the decomposed respiratory and cardiac/heartbeat components, respectively.

2.3. Short Time Cepstral Transform (STCT)

To estimate the IHR, i.e. the IF of the extracted cardiac component, a TF representation should be investigated. As a classic TF representation, the definition of STFT is given as:

$$V_f^{(h)}(t, \xi) = \int f(\tau) h(\tau - t) e^{-i2\pi \xi(\tau - t)} d\tau, \quad (3)$$

where, h is the window function, t indicates time and ξ indicates frequency.

Combining STFT and cepstrum, the signal local oscillatory behavior can be better captured. So the so called short time cepstral transform (STCT) can be defined as [15]:

$$C_f^{(h, \gamma)}(t, q) := \int g_\gamma(V_f^{(h)}(t, \xi)) e^{-i2\pi q \xi} d\xi, \quad (4)$$

where q is called quefrequency, and g_γ is the root function approximating the logarithm function. Since the cepstrum provides the information about periodicity, we call $C_f^{(h, \gamma)}(t, q)$ a TPT of signal f .

2.4. de-shape STFT

In a harmonic series associated with multiples of the fundamental frequency ξ_1 , we should find a sequence of peaks/ridges in the TF representation denoted as $\{\xi_1, 2\xi_1, \dots, N\xi_1\}$. This sequence is called the sub-harmonic series associated with the fundamental frequency ξ_1 . Fig. 3 shows the fundamental and sub harmonics in the frequency domain, which motivates a combination of the STFT and iSTCT $U_f^{(h, \gamma)}(t, \xi) := C_f^{(h, \gamma)}(t, \mathcal{I}\xi)$ to extract the fundamental harmonics called de-shape STFT, defined as [14, 15]:

$$W_f^{(h, \gamma)}(t, \xi) := V_f^{(h)}(t, \xi) U_f^{(h, \gamma)}(t, \xi). \quad (5)$$

Since the harmonic series associated with multiples of the fundamental frequency ξ_1 in $V_f^{(h)}(t, \xi)$ overlaps with the sub-harmonic series associated with multiples of the fundamental frequency ξ_1 in $U_f^{(h, \gamma)}(t, \xi)$ only at ξ_1 , by multiplying $V_f^{(h)}(t, \xi)$ and $U_f^{(h, \gamma)}(t, \xi)$, only the information associated with ξ_1 is left. Thus, the influences caused by the non-trivial sub-harmonics in the TF domain are removed.

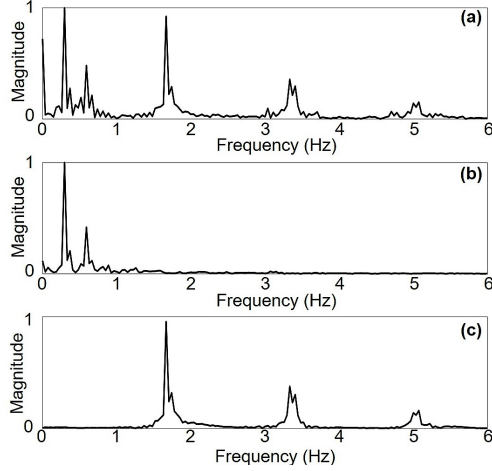


Fig. 3. Spectra of (a) Raw PPG signal with decomposed (b) Respiratory and (c) Cardiac components. Note that either respiratory or cardiac component has more than one harmonics.

2.5. de-shape SST

The SST of STFT ($V_f^{(h)}(t, \xi)$) is defined as [17]:

$$SV_f^{(h,v)}(t, \xi) = \int V_f^{(h)}(t, \eta) \frac{1}{\alpha} g\left(\frac{|\xi - \Omega_f^{(h,v)}(t, \eta)|}{\alpha}\right) d\eta, \quad (6)$$

where $\Omega(\cdot)$ denotes the frequency reassignment vector. Thus, we can define the de-shape SST as [15]:

$$SW_f^{(h,\gamma,v)}(t, \xi) = \int W_f^{(h,\gamma)}(t, \eta) \frac{1}{\alpha} g\left(\frac{|\xi - \Omega_f^{(h,v)}(t, \eta)|}{\alpha}\right) d\eta. \quad (7)$$

With the de-shape SST, the TF representation is further sharpened. Thus, in this paper, we combine the NHA and de-shape SST to study the PPG signal, as shown in Fig. 1.

3. EXPERIMENTS

We apply the proposed approach to a PPG record from the Capnabase dataset¹. The PPG signal is recorded from a subject without any motion with a 300 Hz sampling frequency.

Fig. 4a shows raw PPG data, the same as those shown in Fig. 2a. Fig. 4b and Fig. 4c show the STFT and SST, respectively. With a good correspondence of the spectrum shown in Fig. 3a, there are harmonic spectra on both STFT and SST. Though SST has a higher TF resolution than STFT, according to Equation (6), the frequency reassignment operation does not suppress any sub-harmonics. Fig. 4d shows the de-shape SST result. Ideally, there should be no sub-harmonics left in the de-shape SST. However, sub-harmonics remain, probably because the constructive and destructive interactions among different intrinsic oscillatory modes. From Fig. 2, we know

¹<http://www.capnabase.org>

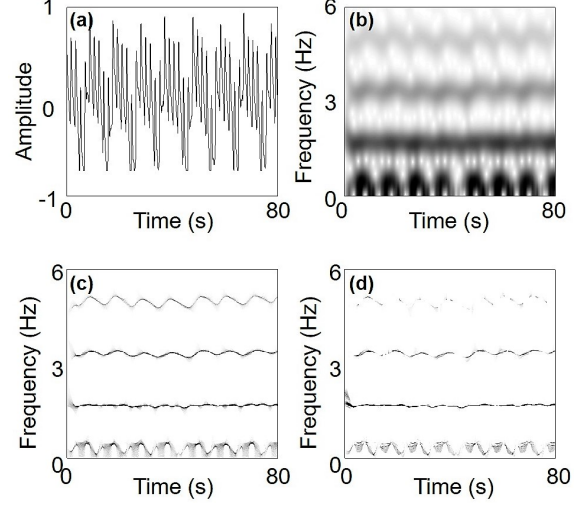


Fig. 4. (a) Raw PPG signal with its (b) STFT, (c) SST and (d) deshape-SST expressions. Note that the traditional deshape-SST cannot fully suppress the sub-harmonics.

there are two kinds of oscillations in the PPG signal: the faster oscillations associated with the heartbeat and the slower ones associated with respiration. The de-shape SST can suppress the sub-harmonics generated either from respiration or heartbeat, but if these two are constructively and destructively combined, the sub-harmonics will not be as supposed.

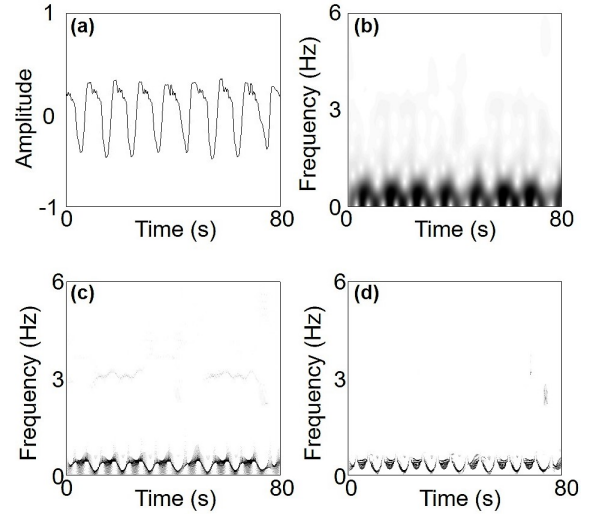


Fig. 5. (a) Extracted respiratory component with its (b) STFT, (c) SST and (d) deshape-SST expressions.

Thus, we propose to first extract the IMs, then the sub-harmonics could be suppressed, and the instantaneous attributes can be accurately estimated. Fig. 5a is the extracted respiration component, the same as Fig. 2b, which shows the low frequency component. Fig. 5b and Fig. 5c demonstrate the STFT and SST results, respectively. Fig. 5d shows the

de-shape SST, and the TF representation is clearer as the energies around 3 Hz are suppressed.

Fig. 6a displays the extracted cardiac/heartbeat component, the same as Fig. 2c. Fig. 6b and Fig. 6c demonstrate the STFT and SST results, respectively, showing the sub-harmonics as expected, since there is no operation in them to remove the sub-harmonics, as shown in Fig. 3c. Fig. 6d shows the de-shape SST, and the sub-harmonics are suppressed compared with Fig. 6c. Thanks to the NHA, the extracted heartbeat component has a set of more regular harmonics, which can be successfully removed using de-shape SST, while the complicated harmonics in Fig. 4c cannot be removed.

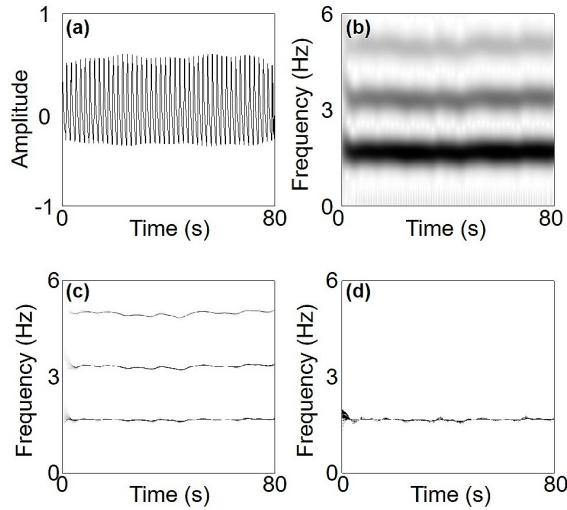


Fig. 6. (a) Extracted cardiac component with its (b) STFT, (c) SST and (d) deshape-SST expressions.

To estimate the IHR from the TPT, we employ a ridge extraction method [15] to directly obtain the IHR number. Fig. 7a shows the extracted energies from the de-shape SST representation in Fig. 4d. Because the sub-harmonics are not suppressed, more than one components can be extracted. Fig. 7b shows the IHR plot extracted from our result shown in Fig. 6d, where only the true IHR is extracted.

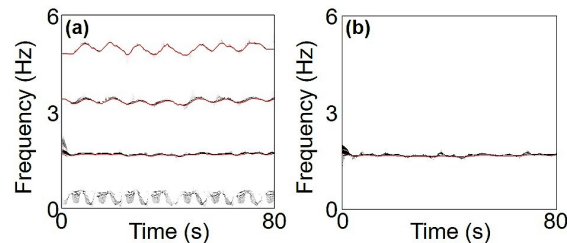


Fig. 7. IHRs estimated from (a) de-shape SST and (b) the proposed method.

Fig. 8 shows IHRs estimated from the reference ECG record in the same database. Fig. 8a shows the de-shape SST of the ECG, while Fig. 8b demonstrates the extracted

IHR. Since, we do not apply our method to the ECG record, there are two instantaneous components highlighted. Table 1 displays the quantitative comparisons of the IHRs from the traditional de-shape SST, our method on PPG data as well as IHRs extracted from the reference ECG data. Note that IHRs of the first mode from the de-shape SST of PPG and ECG are around 1.66Hz~1.7Hz, which are close to that from the “only” mode extracted from the proposed method. In addition, the estimate from our method has a smaller standard deviation, resulting in a smooth IHR, which is expected because the raw PPG data have the constructive and deconstructive interferences from cardiac and respiration components, and our approach suppresses them.

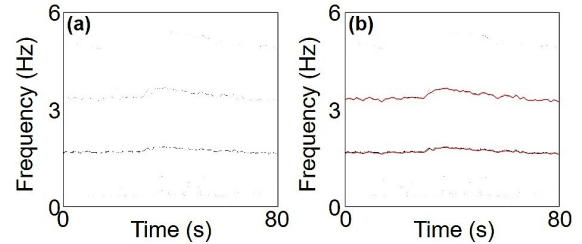


Fig. 8. (a) de-shape SST of an associated ECG record and (b) the corresponding IHR estimation.

Table 1. IHR estimates using de-shape SST, our proposed method and the estimates from ECG data. (Unit: Hz.)

	de-shape SST on PPG		
mean	1.6601	3.3151	4.9557
std	0.0229	0.0572	0.1104
	<i>1st mode</i>	<i>2nd mode</i>	<i>3rd mode</i>
	reference ECG		Proposed Method
mean	1.7007	3.4030	1.6617
std	0.0558	0.1117	0.0218
	<i>1st mode</i>	<i>2nd mode</i>	<i>Only mode</i>

4. CONCLUSION

In this paper, we propose a hybrid IHR estimation method based on NHA and de-shape SST. Without NHA, the traditional de-shape SST cannot remove the complicated harmonics generated by different intrinsic oscillatory components. Without de-shape SST, it is difficult to estimate IHR directly from a TF domain. The preliminary results demonstrate that the proposed approach is promising for IHR estimation from PPG data. From our observations, the proposed method may also contribute to other biomedical data, such as ECG/EKG. In addition, our work indicates the potential of simultaneously obtaining IHR and instantaneous respiratory rate from the PPG signal. Compared with IHR, the low-frequency mode is more complicated, so the physiological and clinical significance warrants further investigation.

5. REFERENCES

- [1] L. Nilsson, A. Johansson, and S. Kalman, "Monitoring of respiratory rate in postoperative care using a new photoplethysmographic technique," *Journal of clinical monitoring and computing*, vol. 16, no. 4, pp. 309–315, 2000.
- [2] B. Sun, H. Feng, and Z. Zhang, "A new approach for heart rate monitoring using photoplethysmography signals contaminated by motion artifacts," in *Acoustics, Speech and Signal Processing (ICASSP), 2016 IEEE International Conference on*. IEEE, 2016, pp. 809–813.
- [3] A. Ukil, S. Bandyopadhyay, C. Puri, and A. Pal, "Heart-trend: an affordable heart condition monitoring system exploiting morphological pattern," in *Acoustics, Speech and Signal Processing (ICASSP), 2016 IEEE International Conference on*. IEEE, 2016, pp. 6260–6264.
- [4] H. Yang, "Multiresolution mode decomposition for adaptive time series analysis," *arXiv preprint arXiv:1709.06880*, 2017.
- [5] A. Temko, "PPG-based heart rate estimation using wiener filter, phase vocoder and viterbi decoding," in *Acoustics, Speech and Signal Processing (ICASSP), 2017 IEEE International Conference on*. IEEE, 2017, pp. 1013–1017.
- [6] K. V. Madhav, M. R. Ram, E. H. Krishna, N. R. Komalla, and K. A. Reddy, "Estimation of respiration rate from ECG, BP and PPG signals using empirical mode decomposition," in *Instrumentation and Measurement Technology Conference (I2MTC), 2011 IEEE*. IEEE, 2011, pp. 1–4.
- [7] H.-T. Wu, Y.-H. Chan, Y.-T. Lin, and Y.-H. Yeh, "Using synchrosqueezing transform to discover breathing dynamics from ECG signals," *Applied and Computational Harmonic Analysis*, vol. 36, no. 2, pp. 354–359, 2014.
- [8] C. Orphanidou, "Derivation of respiration rate from ambulatory ECG and PPG using ensemble empirical mode decomposition: Comparison and fusion," *Computers in biology and medicine*, vol. 81, pp. 45–54, 2017.
- [9] E. Khan, F. Al Hossain, S. Z. Uddin, S. K. Alam, and M. K. Hasan, "A robust heart rate monitoring scheme using photoplethysmographic signals corrupted by intense motion artifacts," *IEEE Transactions on Biomedical Engineering*, vol. 63, no. 3, pp. 550–562, 2016.
- [10] R. W. C. G. R. Wijshoff, A. M. T. M. van Asten, W. H. Peeters, R. Bezemer, G. J. Noordergraaf, M. Mischi, and R. M. Aarts, "Photoplethysmography-based algorithm for detection of cardiogenic output during cardiopulmonary resuscitation," *IEEE Transactions on Biomedical Engineering*, vol. 62, no. 3, pp. 909–921, 2015.
- [11] Y. Sun and N. Thakor, "Photoplethysmography revisited: from contact to noncontact, from point to imaging," *IEEE Transactions on Biomedical Engineering*, vol. 63, no. 3, pp. 463–477, 2016.
- [12] H. Demirezen and C. E. Erdem, "Remote photoplethysmography using nonlinear mode decomposition," in *2018 IEEE International Conference on Acoustics, Speech and Signal Processing (ICASSP)*. IEEE, 2018, pp. 1060–1064.
- [13] E. Gil, P. Laguna, J. P. Mart'inez, O. Barquero-Pérez, A. Garc'ia-Alberola, and L. Sörnmo, "Heart rate turbulence analysis based on photoplethysmography," *IEEE Transactions on Biomedical Engineering*, vol. 60, no. 11, pp. 3149–3155, 2013.
- [14] L. Su and H.-T. Wu, "Extract fetal ecg from single-lead abdominal ecg by de-shape short time fourier transform and nonlocal median," *Frontiers in Applied Mathematics and Statistics*, vol. 3, p. 2, 2017.
- [15] C.-Y. Lin, L. Su, and H.-T. Wu, "Wave-Shape function analysis," *Journal of Fourier Analysis and Applications*, vol. 24, no. 2, pp. 451–505, 2018.
- [16] G. Tang and H. Yang, "A fast algorithm for multiresolution mode decomposition," *arXiv preprint arXiv:1712.09338*, 2017.
- [17] H. Yang, "Synchrosqueezed wave packet transforms and diffeomorphism based spectral analysis for 1D general mode decompositions," *Applied and Computational Harmonic Analysis*, vol. 39, no. 1, pp. 33–66, 2015.